

Quasi-two-dimensional electron gas at metallic densities

B. Bernu,¹ F. Delyon,² and M. Holzmann^{1,3}¹*LPTMC, UMR 7600 CNRS, Université P. et M. Curie, Paris, France*²*CPHT, UMR 7644 CNRS, École Polytechnique, Palaiseau, France*³*LPMMC, UMR 5493 CNRS, Université J. Fourier, Grenoble, France*

(Received 21 September 2010; published 16 December 2010)

We consider the three-dimensional electron gas confined by a strictly two-dimensional homogeneous positive charge density at $z=0$. Within the Hartree-Fock approximation, we study the mode structure in the confined direction in the metallic regime. We find that for $r_s < 1.3$ ($r_s < 2.5$) the unpolarized (polarized) electron gas starts to populate also the first-excited state in the z direction.

DOI: [10.1103/PhysRevB.82.245116](https://doi.org/10.1103/PhysRevB.82.245116)

PACS number(s): 71.10.Ca, 71.10.Hf, 71.30.+h

I. INTRODUCTION

The two-dimensional homogeneous electron gas (2DEG) is one of the most simple and thus widely used model to study electronic correlations in two dimensions.¹⁻³ Experimentally, two-dimensional electronic systems have been realized using heterostructures, e.g., semiconductor-insulator interfaces, where layers of electrons are tightly confined in one spatial dimension (z) by strong surface electric fields and the discreteness of the quantized energy levels in z becomes important.⁴ However since electronic wave functions and electromagnetic fields spatially extend in the z direction, theoretical predictions for the 2DEG must be modified before a quantitative comparison is possible.⁵

In order to study general effects due to the interplay of electron-electron interactions and correlations with the finite extension of the electronic density in the z direction, we introduce the model of a quasi-2DEG (Q2DEG). This model provides a simple and natural extension of the 2DEG which contains essential features of more sophisticated microscopic descriptions of heterostructures.⁴ Frequently, experiments are modeled with additional parameters to account for the finite thickness. In general, these parameters should not be considered as independent of the density due to charge neutrality.

Similar to the electron gas in two and three dimensions (3D), we consider a jellium of electrons in a positive charged background insuring total charge neutrality. Whereas the electrons are treated fully three dimensional, the background charges remain strictly two dimensional, described by a homogeneous charge density, σ_0 , in the plane $z=0$. For vanishing total charge of the system, the electrons are confined around the plane $z=0$. Similar to the 2DEG, we introduce the dimensionless parameter $r_s = 1/(a_B \sqrt{\pi \sigma_0})$, where $a_B = \hbar^2/(m_e e^2)$ is the Bohr radius, m_e the mass, and $(-e)$ the charge of the electron. At zero temperature, the system is fully described by the value of r_s , which characterizes the effective two-dimensional density of the electrons.

In this paper, we study the Q2DEG in the metallic density region ($0.5 \leq r_s \leq 5$) in the Hartree-Fock (HF) approximation. In particular, we determine the spatial density distribution of the electrons in the z direction and the possible transition between the occupation of a single confined mode to the occupation of two or more excited modes or subbands, in z . We show that for $r_s \rightarrow 0$ the energy per particle can be written as

$$E_m(c_a, r_s) = \frac{K_p}{r_s^2} \sum_{a=1}^m c_a^2 + \frac{\mathcal{E}_m(c_a, r_s)}{r_s^{4/3}} + \frac{\mathcal{X}_m(c_a, r_s)}{r_s} + \mathcal{C}_m(c_a, r_s), \quad (1)$$

where m is the number of occupied modes in the z direction and \mathcal{E}_m and \mathcal{X}_m are smooth functions of r_s , determined within HF, K_p is a constant for fixed spin polarization, p , and c_a are the concentrations of electrons in each mode. The correlation energy beyond Hartree-Fock, \mathcal{C}_m , is estimated within density-functional theory. At fixed density (fixed r_s), we determine the ground state for given concentrations, c_a , and, finally, minimize with respect to the concentrations to obtain $E_m(c_{a,\min}, r_s)$. The main goal of this paper is to determine the density where the two-mode solution (Sec. V) becomes energetically favorable compared to the single-mode solution.

The paper is organized as follows: Sec. II introduces the model Hamiltonian of the Q2DEG and discusses the technical problems related to the thermodynamic limit and the long-range behavior of the Coulomb $1/r$ potential in the potential energy. In Sec. III, we use the HF approximation to simplify the many-body problem and discuss the general structure of the ground-state energy in the high-density limit, $r_s \rightarrow 0$. In the following sections: Secs. IV and V, we discuss the single-mode and two-mode solutions of the HF approximation. For both cases, we first start discussing the Hartree approximation, where we have found analytical solutions for the resulting nonlinear Schrödinger equation. These solutions serve to obtain a first estimate for the Hartree and exchange contribution to the energy, \mathcal{E}_m^0 and \mathcal{X}_m^0 , respectively. We will show later that the numerical minimization of the full HF energy introduces only minor corrections. Finally, we briefly discuss correlation effects beyond HF within the local-density approximation (LDA) using density-functional theory (Sec. VI).

II. QUASI-TWO-DIMENSIONAL ELECTRON-GAS MODEL

Let us consider N electrons interacting with a homogeneous positive charged, strictly two-dimensional plane at $z=0$ and area $S=L^2$. Assuming a charge-neutral system, the background surface density writes $\sigma_0=N/S$. The N -body Hamiltonian is given by

$$\mathcal{H}_N = \sum_{i=1}^N -\frac{\hbar^2}{2m_e} \Delta_i + V_N, \quad (2)$$

where V_N is the total potential energy of all charges.

It is well known that the Coulomb potential poses difficulties in the definition of the potential energy in the thermodynamic limit due to the nonintegrability at infinity. The local singularity of the Coulomb potential near the origin is a classical problem of self-adjointness and here we only focus on the definition of the potential with periodic boundary conditions.

Let Λ denotes the two-dimensional lattice in \mathbb{R}^3 generated by the vectors $(L, 0, 0)$ and $(0, L, 0)$. For a regular integrable interaction v , we formally define the total periodic potential as

$$V_N = V_{ee} + V_{eb} + V_{bb}, \quad (3)$$

$$V_{ee} = \frac{1}{2} \sum_{i \neq j, \tau \in \Lambda} v(R_i - R_j + \tau) + \frac{1}{2} \sum_i \sum_{\tau \in \Lambda, \tau \neq 0} v(\tau), \quad (4)$$

$$V_{eb} = -\frac{N}{S} \sum_i \int_{\mathbb{R}^2} dr v(R_i - r), \quad (5)$$

$$V_{bb} = \frac{N^2}{2S^2} \int_{S \times \mathbb{R}^2} dr dr' v(r - r'), \quad (6)$$

where the index e holds for the electrons and b holds for the positive background. The last term in Eq. (4) is the interaction of an electron with all its periodized images. As soon as the interaction v is regular and integrable, we can rewrite the potential energy as

$$V_N = \frac{1}{2} \sum_{i \neq j} \left[\hat{v}(R_i - R_j) + \frac{1}{S} v_1(z_i - z_j) \right] - \sigma_0 \sum_i v_1(z_i) + \frac{N}{2} C_v \quad (7)$$

with

$$\hat{v}(R) = \sum_{\tau \in \Lambda} \left[v(R + \tau) - \frac{1}{S} \int_S dr v(R + \tau + r) \right], \quad (8)$$

$$v_1(z) = \int_{\mathbb{R}^2} dr v[(r, z)] - v[(r, 0)], \quad (9)$$

and C_v is the Madelung energy of electrons on the lattice Λ in a homogeneous background,

$$C_v = \sum_{\tau \in \Lambda, \tau \neq 0} \left[v(\tau) - \frac{1}{S} \int_S dr v(r + \tau) \right] - \frac{1}{S} \int_S dr v(r). \quad (10)$$

Let us notice that the Fourier transform $\tilde{v}(K)$ of \hat{v} is directly related to the Fourier transform, $\bar{v}(K)$, of v . As can be directly verified, we have $\tilde{v}(K) = \bar{v}(K)$, except that $\tilde{v}(K) = 0$ for $k_x = k_y = 0$. With this new definition [Eq. (7)], we only need that \hat{v} , v_1 , and C_v are well defined, i.e.,

$$\sum_{\tau \in \Lambda} \left| v(R + \tau) - \frac{1}{S} \int_S dr v(R + \tau + r) \right| < +\infty \quad (11)$$

$$\int_{\mathbb{R}^2} dr |v[(r, z)] - v[(r, 0)]| < +\infty \quad (12)$$

These conditions are fulfilled by the Coulomb potential $v_C(R) = e^2/R$, except at $R=0$ as mentioned above. Furthermore, we have $v_1(z) = -2\pi e^2|z|$ and $\tilde{v}(K) = 4\pi e^2/(k_x^2 + k_y^2 + k_z^2)$ for $k_x \neq 0$ or $k_y \neq 0$ and 0 otherwise, and the periodic potential energy, Eq. (7), finally writes

$$V_N = \frac{e^2}{2} \sum_{i \neq j} \left[v^{q2D}(R_{ij}) - \frac{2\pi|z_i - z_j|}{S} \right] + 2\pi e^2 \sigma_0 \sum_i |z_i| + \frac{N}{2} C_v, \quad (13)$$

$$v^{q2D}(R) = \frac{1}{S} \sum_{k \neq 0} \int \frac{dk_z}{2\pi} \frac{4\pi}{k^2 + k_z^2} e^{iK \cdot R} \quad (14)$$

where $K = (k, k_z)$ and $e^{ik \cdot \tau} = 1$ for $\tau \in \Lambda$.

III. HARTREE-FOCK APPROXIMATION

Within the HF approximation we minimize the ground-state energy per particle, E , with respect to variations in the many-body wave function, $\Psi_N = \det\{\Psi_{i\uparrow}\} \det\{\Psi_{i\downarrow}\}$, in the subspace of single Slater determinants

$$E = \frac{1}{N} \frac{\langle \Psi_N | \mathcal{H}_N | \Psi_N \rangle}{\langle \Psi_N | \Psi_N \rangle} \quad (15)$$

In the following, we assume that $\{\Psi_{i\sigma}\}$ ($\sigma = \uparrow, \downarrow$) are normalized, orthogonal single-particle wave functions, and we obtain for the total energy per particle

$$\begin{aligned} E = & -\frac{1}{N} \sum_{i\sigma} \int_{S \times \mathbb{R}} dR \Psi_{i\sigma}^*(R) \frac{\hbar^2}{2m_e} \Delta \Psi_{i\sigma}(R) \\ & + \frac{1}{N} \frac{e^2}{2} \int_{S \times \mathbb{R}} dR dR' n_e(R) v^{q2D}(R - R') n_e(R') \\ & - \frac{1}{N} \frac{e^2}{2} \sum_{i,j,\sigma} \int_{S \times \mathbb{R}} dR dR' \Psi_{i\sigma}^*(R) \Psi_{j\sigma}(R) v^{q2D}(R - R') \\ & \times \Psi_{i\sigma}(R') \Psi_{j\sigma}^*(R') + \frac{1}{N} \int_{S \times \mathbb{R}} dR n_e(R) 2\pi e^2 \sigma_0 |z| \\ & - \frac{\pi e^2}{NS} \int_{S \times \mathbb{R}} dR dR' n_e(R) |z - z'| n_e(R') \\ & + \frac{\pi e^2}{NS} \sum_{i,j,\sigma} \int_{S \times \mathbb{R}} dR dR' \Psi_{i\sigma}^*(R) \Psi_{j\sigma}(R) \\ & \times |z - z'| \Psi_{i\sigma}(R') \Psi_{j\sigma}^*(R') + \frac{C_v}{2} \end{aligned} \quad (16)$$

where we have defined the total electronic density by

$$n_e(R) = \sum_{i\sigma} |\Psi_{i\sigma}(R)|^2 \quad (17)$$

In this paper, we are interested in a quasi-two-dimensional regime, where we expect that the electrons populate a finite number, m , of discrete modes in the z direction, whereas the density of states is continuous in the plane at constant z , in the thermodynamic limit. Each single-body wave function $\Psi_{i\sigma}$ is then taken as a product of a plane wave ϕ_k in the plane $z=0$ and a wave function ψ_a in the z direction, where a labels the mode. Let N_a be the number of electrons in the mode a and $c_a=N_a/N$, $N=\sum_a N_a$. Accounting for the spin polarization p of the electrons, we have $N_a=N_{a\uparrow}+N_{a\downarrow}$ and $c_a=c_{a\uparrow}+c_{a\downarrow}$. In the following, we restrict the discussion to (i) the fully polarized gas ($p=1$), where $c_a=c_{a\uparrow}$ and $c_{a\downarrow}=0$ and (ii) the unpolarized electron gas ($p=0$) with $c_{a\uparrow}=c_{a\downarrow}=c_a/2$ (unpolarized in each mode a). We further assume that the wave functions do not depend on spin: $\psi_{a\sigma}\equiv\psi_a$.

In each mode a, σ , all transverse plane waves are occupied up to $k_{F_{a\sigma}}=\sqrt{c_{a\sigma}}k_F$ with $k_{F_{a\sigma}}=2/r_s$, and, in the thermodynamic limit, all summations over transverse states are replaced by integrals inside the Fermi surfaces

$$\sum_{i\sigma} \equiv \sum_{a\sigma} \sum_{|k|<k_{F_{a\sigma}}} \rightarrow \sum_{a\sigma} \frac{N}{\pi k_F^2} \int_{|k|<k_{F_{a\sigma}}} d^2k. \quad (18)$$

Further, for $N\rightarrow\infty$, the last line of Eq. (16) vanishes.

It is instructive to regroup the different contributions to the total energy (in Hartree) as follows:

$$E[c_a, \psi_a, r_s] = \frac{K_p \sum_a c_a^2}{r_s^2} + \frac{\mathcal{E}[c_a, \psi_a]}{r_s^{4/3}} + \frac{\mathcal{X}[c_a, \psi_a, r_s]}{r_s} \quad (19)$$

where the first term is the in plane, strictly two dimensional, kinetic energy with $K_0=1/2$ for the unpolarized and $K_1=1$ for the polarized electron gas. In order to separate the explicit r_s dependency in the following two terms, we introduce $u=r_s^{1/3}k_F z$ together with the normalization $\int_{\mathbb{R}} du |\psi_{a\sigma}(u)|^2 = 1$ of the confined modes. All contributions independent of the in-plane modes are contained in \mathcal{E}

$$\begin{aligned} \mathcal{E}[c_a, \psi_a] = & -2 \sum_a c_a \int_{\mathbb{R}} du \psi_a(u) \psi_a''(u) + \int_{\mathbb{R}} du \rho(u) \frac{|u|}{2} \\ & + \int_{\mathbb{R}} du \rho(u) v_\rho(u) \end{aligned} \quad (20)$$

where the electrostatic potential, v_ρ , is determined by the one-dimensional Poisson equation,

$$v_\rho''(u) = \delta(u) - \rho(u) \quad (21)$$

from the total electronic density distribution $\rho(u) = \sum_{a\sigma} c_{a\sigma} |\psi_{a\sigma}|^2 = \sum_a c_a |\psi_a|^2$ and the positive background charges at $z=0$. Using $v_\rho(\infty) = v_\rho'(\infty) = 0$, we have

$$v_\rho(u) = \frac{|u|}{2} - \frac{1}{2} \int_{\mathbb{R}} du' \rho(u') |u - u'| \quad (22)$$

The exchange term, \mathcal{X} , explicitly mixes transverse and confined states,

$$\mathcal{X}[c_a, \psi_a, r_s] = - \sum_{a,b} \frac{r_s^{1/3}}{4\pi} \int_{\mathbb{R}} dv |\tilde{\rho}_{ab}(v)|^2 \tilde{Y}(c_a, c_b, r_s^{1/3} G_p v) \quad (23)$$

where $\tilde{\rho}_{ab}(v) = \int_{\mathbb{R}} du \rho_{ab}(u) \exp(-iv u)$, $\rho_{ab}(u) = \psi_a(u) \psi_b(u)$, $G_0 = \sqrt{2}$ (unpolarized), and $G_1 = 1$ (polarized). The exchange function \tilde{Y} (see Appendix A) is given by,

$$\tilde{Y}(c_a, c_b, v) = \frac{2}{\pi^2} \int_{|k|^2 < c_a} d^2k \int_{|k'|^2 < c_b} d^2k' \frac{1}{|k - k'|^2 + v^2},$$

and introduces a smooth variation in \mathcal{X} as a function of r_s .

The Hartree-Fock ground state is determined by minimizing the total energy, Eq. (19), with respect to p , c_a , and ψ_a , at fixed density, r_s . We simplify this rather complex optimization problem by considering only the completely polarized or unpolarized electron gas. For fixed concentrations, c_a , the minimum of E with respect to ψ_a is independent from the in-plane kinetic energy. From the formal variation in the energy with respect to ψ_a we obtain

$$\frac{dE}{d\psi_a} = \frac{4}{r_s^{4/3}} \mathcal{H}_0 c_a \psi_a + \frac{4}{r_s} \sum_b V_{a,b}^{\text{exc}}(u) \psi_b, \quad (24)$$

$$\mathcal{H}_0 = -\partial_u^2 + v_\rho(u), \quad (25)$$

$$V_{a,b}^{\text{exc}}(u) = -\frac{r_s^{1/3}}{4\pi} \int_{\mathbb{R}} dv \tilde{\rho}_{ab}(v) \tilde{Y}(c_a, c_b, r_s^{1/3} G_p v) e^{i v u}. \quad (26)$$

In the limit of small r_s , the exchange energy is negligible and the wave functions, $\psi_a \equiv \psi_a^0$, are entirely determined by minimizing \mathcal{E} , or, equivalently by the Hartree equation

$$\mathcal{H}_0 \psi_a^0 = -\lambda_a \psi_a^0, \quad (27)$$

which leads to

$$E_m^0 = \frac{K_p}{r_s^2} \sum_a c_a^2 + \frac{\mathcal{E}_m^0}{r_s^{4/3}} + \frac{\mathcal{X}_m^0}{r_s}, \quad (28)$$

where, $\mathcal{X}_m^0 \equiv \mathcal{X}[c_a, \psi_a^0, r_s]$ and

$$\mathcal{E}_m^0 \equiv \mathcal{E}[c_a, \psi_a^0] = -2 \sum_a c_a \lambda_a - v_\rho(0) - \int_{\mathbb{R}} du \rho(u) v_\rho(u) \quad (29)$$

are independent of r_s . This provides us with a semianalytical approximation for the total energy, E_m^0 , which appears to be very close to the full minimization of the energy including exchange, E_m , for the densities considered. Whereas the in-plane kinetic energy term does not influence the shape of the distribution in z , it favors multimode occupation in the high-density limit, $r_s \rightarrow 0$.

IV. SINGLE-MODE SOLUTION

For a single mode, we minimize Eq. (19) with $\rho(u) = \psi_0^2(u)$ ($c_0=1$) so that ψ_0 satisfies the nonlinear Schrödinger equation, Eq. (24),

$$(\mathcal{H}_0 + r_s^{1/3} V_{00}^{exc})\psi_0 = -\lambda_0\psi_0, \quad (30)$$

and we obtain

$$E_1 = \frac{K_p}{r_s^2} + \frac{\mathcal{E}_1}{r_s^{4/3}} + \frac{\mathcal{X}_1}{r_s}, \quad (31)$$

where \mathcal{E}_1 and \mathcal{X}_1 are the values of the Hartree and exchange term using the optimal ψ_0 .

For the strictly two-dimensional electron gas, we have $\rho^{(2D)}(u) = \delta(u)$. Neglecting the zero-point energy of the confinement, \mathcal{E}_1 , in this limit, and using $\int_{\mathbb{R}} d\nu \tilde{Y}(1, 1, \nu) = 32/3$, we recover $E^{(2D)}(p=0) = 1/(2r_s^2) - 8/(3\pi r_s \sqrt{2})$ for the unpolarized and $E^{(2D)}(p=1) = 1/r_s^2 - 8/(3\pi r_s)$ for the polarized electron gas.

A. Hartree solution without exchange, \mathcal{E}_1^0

We determine the one-mode solution of the Hartree equation, Eq. (30) with $V_{00}^{exc} = 0$, which determines the density distribution of the mode with $\lambda_0 > 0$ in the high-density region, $r_s \rightarrow 0$. Assuming $\psi_0(u)$ to be an even function of u , we restrict the discussion to $u > 0$ in the following. From the leading-order behavior X_0 of the solution at large u , where $v_\rho(u)$ vanishes, we use a series in X_0 as ansatz for $\psi(u)$,

$$X_0 = \sqrt{f_0} e^{-\alpha u}, \quad (32)$$

$$\psi_0(u) = \alpha^2 \sum_{k \geq 0} (-1)^k a_k X_0^{2k+1}, \quad (33)$$

where $\alpha = \sqrt{\lambda_0}$, f_0 , and a_k are to be determined ($a_0 = 1$). The density is then given by,

$$\rho(u) = \alpha^4 \sum_{k \geq 0} (-1)^k \rho_k X_0^{2k+2} \quad \text{with} \quad \rho_k = \sum_{j=0}^k a_j a_{k-j}, \quad (34)$$

and the potential is obtained by integrating twice $v_\rho''(u) = -\rho(u)$ for $u > 0$ with the conditions $v_\rho(\infty) = 0$ and $v_\rho'(\infty) = 0$,

$$v_\rho(u) = -\alpha^2 \sum_{k \geq 0} (-1)^k v_k X_0^{2k+2} \quad \text{with} \quad v_k = \frac{\rho_k}{4(k+1)^2}, \quad (35)$$

and

$$\psi_0''(u) = \alpha^4 \sum_k (-1)^k a_k (2k+1)^2 X_0^{2k+1}, \quad (36)$$

$$v_\rho(u)\psi_0(u) = -\alpha^4 \sum_{k \geq 0} (-1)^k w_k X_0^{2k+3} \quad \text{with} \quad w_k = \sum_{j=0}^k v_j a_{k-j}. \quad (37)$$

Thus, imposing $\psi_0'' - (v_\rho + \alpha^2)\psi_0 = 0$ leads to the equation

$$0 = \alpha^4 X_0 \left[\sum_{k \geq 0} (-1)^k a_k [(2k+1)^2 - 1] X_0^{2k} + \sum_{k \geq 0} (-1)^k w_k X_0^{2k+2} \right]. \quad (38)$$

From the definition $a_0 = 1$, we get $\rho_0 = 1$, $v_0 = \frac{1}{4}$, and $w_0 = \frac{1}{4}$. The other terms are obtain by recurrence

TABLE I. Parameters and various quantities of the single-mode solution of the Hartree equation without exchange term.

f_0	15.5610024546998
α	0.465180466326271
λ_0	0.216392866251527
$v(0)$	-0.674164469749883
$\psi_0(0)$	0.522553284700250
$\langle v \rangle$	-0.307947186951202
$\langle -\Delta \rangle$	0.0915543206996701
\mathcal{E}_1^0	0.549325924198031

$$a_k = \frac{w_{k-1}}{4k(k+1)}. \quad (39)$$

With these definitions all coefficients a_k , ρ_k , v_k , and w_k are positive. The two parameters α and f_0 are determined by imposing $\psi_0'(0) = 0$ and the normalization

$$0 = \sum_{k \geq 0} (-1)^k (2k+1) a_k f_0^k \psi_0'(0), \quad (40)$$

$$\frac{1}{2} = \alpha^3 \sum_{k \geq 0} \frac{(-1)^k \rho_k f_0^{k+1}}{2(k+1)} = \int_0^\infty du \psi_0^2(u). \quad (41)$$

The numerical results are given in Table I, together with the values of the different contributions to the Hartree energy. In particular, from Eqs. (25) and (27), we have $\lambda_0 = \alpha^2 = -(\langle -\Delta \rangle + \langle v_\rho \rangle)$ and from Eq. (29), we have $\mathcal{E}_1^0 = -2\lambda_0 - v_\rho(0) - \langle v_\rho \rangle$ with $\langle v_\rho \rangle = \int_{\mathbb{R}} du \rho(u) v_\rho(u) = -\alpha^5 \sum_{k \geq 0} (-1)^k \tau_k f_0^{k+2} / (k+2)$, $\tau_k = \sum_{j=0}^k \rho_j v_{k-j}$, and the kinetic energy writes $\langle -\Delta \rangle = \langle \psi_0 | -\partial_u^2 | \psi_0 \rangle = \alpha^5 \sum_{k \geq 0} \tau_k' (-f_0)^{k+1} / (k+1)$ with $\tau_k' = \sum_{j=0}^k (2j+1)^2 a_j a_{k-j}$. Notice that \mathcal{E}_1^0 is independent of the polarization.

B. One-mode exchange energy in the Hartree approximation, \mathcal{X}_1^0

From the Fourier transform, $\tilde{\rho}(v)$, of the ground-state density, $\rho_0 = \psi_0^2$, obtained from the Hartree equation, we can estimate the exchange contribution, Eq. (23), to the total energy. Since we have $\tilde{Y} > 0$ and $0 < \tilde{\rho}(v) < 1$, the exchange energy of the quasi-two-dimensional gas is greater than its strictly two-dimensional value obtained with $\tilde{\rho}^{(2D)}(v) = 1$.

The main contribution of the exchange integral comes from the logarithmic singularity of the integrand at $v=0$; details on the numerical evaluation are given in Appendix B and the results for the total energy are shown in Fig. 1. For densities corresponding to $0.5 \leq r_s \leq 5$, the exchange integral, \mathcal{X}_1^0 , is well approximated by $\mathcal{X}_1^0(p=1, r_s) \approx -0.4356 - 0.06127 \ln(r_s)$ for the polarized gas.

Within the Hartree approximation, $\tilde{\rho}(v)$ is independent of r_s and polarization, p , so that a simple relation between \mathcal{X}_1^0 of the polarized and unpolarized electron gas at different r_s can be established,

$$\mathcal{X}_1^0(p=0, r_s) = \frac{\mathcal{X}_1^0(p=1, 2\sqrt{2}r_s)}{\sqrt{2}}. \quad (42)$$

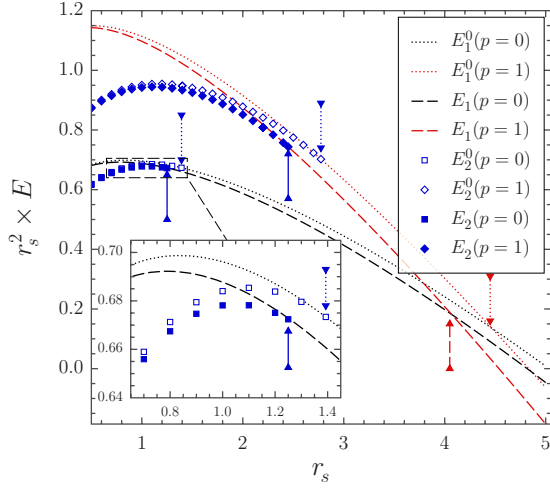


FIG. 1. (Color online) Comparison of the energies of the Q2DEG in the different phases within HF: black for the single-mode unpolarized ($p=0$) electron gas, red for the single-mode polarized ($p=1$) electron gas and blue for two occupied excited modes in z . For each phase we compare the HF energy using the Hartree density profile in z with the full HF minimization: dashed (respectively, dotted) lines stand for E_1 (respectively, E_1^0) of the single-mode solution from Eq. (43) [respectively, Eq. (28)], filled (respectively, open) symbols stand for the energies including two occupied modes, E_2 (respectively, E_2^0) from Eq. (55) [respectively, Eq. (54)], with squares (respectively, diamonds) for the unpolarized (respectively, polarized) gas. The red arrows indicate the transition between the unpolarized gas and the polarized gas at $r_s \approx 4.45$ in the approximation using the Hartree density profile; minimization of the full HF energies shifts the transition to slightly higher density, $r_s \approx 4.05$. Blue arrows indicate the transitions from the single-mode system to two occupied excited modes increasing the density. The inset shows the transition region of the unpolarized gas.

Using our approximate expression for $\mathcal{X}_1^0(p=1, r_s)$ together with Eq. (42) in Eq. (31), we can estimate that for $r_s \gtrsim 4.56$ the polarized phase is energetically favorable compared to the unpolarized phase.

C. Full minimization

The full minimization assuming a single mode is done numerically (see Appendix C for the numerical details), and we have

$$E_1 = \frac{K_p}{r_s^2} + \frac{\mathcal{E}_1(r_s)}{r_s^{4/3}} + \frac{\mathcal{X}_1(r_s)}{r_s}, \quad (43)$$

where \mathcal{E}_1 and \mathcal{X}_1 depend on r_s and the polarization, p . Figure 2 illustrates the small improvements due to the full minimization compared to the Hartree approximation, E_1^0 .

V. TWO-MODE SOLUTION

In this section, we look for the ground-state energy with two modes, where the density is given by

$$\rho(u) = (1-c)\psi_0^2(u) + c\psi_1^2(u), \quad (44)$$

and $c \equiv c_1$ is the concentration of the excited mode, ψ_1 . Analogous to the discussion of the single-mode solution, we

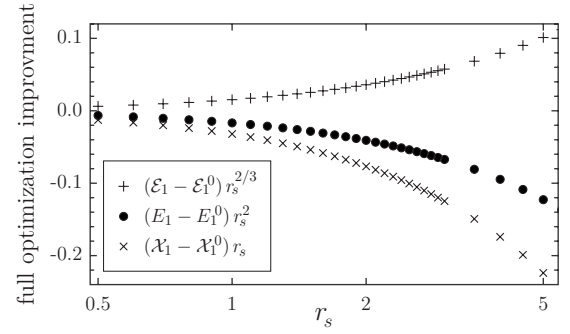


FIG. 2. Importance of the full minimization of all the different components of the HF energy, from Eqs. (29) and (43) for the polarized single-mode gas. Shown are the total energy in Hartree times r_s^2 , together with the Hartree and exchange contributions in the same units. The gain in exchange energy is roughly twice the increase in the Hartree energy.

first minimize the Hartree energy for given c with respect to ψ_0 and ψ_1 to obtain \mathcal{E}_2^0 . Then, we evaluated the exchange term within this solution, \mathcal{X}_2^0 , and, finally, we minimize the full Hartree-Fock energy including the exchange.

A. Two-mode Hartree solution without exchange, \mathcal{E}_2^0

Generalizing the single-mode solution of the previous section, we express the wave functions as series of exponentials. Assuming $\psi_0(u)$ [respectively, $\psi_1(u)$] to be an even (respectively, odd) function of u , we restrict ψ_0 and ψ_1 to non-negative arguments in the following:

$$X_0 = \sqrt{f_0} e^{-\alpha u}, \quad (45)$$

$$X_1 = \sqrt{f_1} e^{-s\alpha u}, \quad (46)$$

$$\psi_0(u) = \frac{\alpha^2}{\sqrt{1-c}} \sum_{k,k' \geq 0} a_{k,k'} X_0^{2k+1} X_1^{2k'}, \quad (47)$$

$$\psi_1(u) = \frac{s^2 \alpha^2}{\sqrt{c}} \sum_{k,k' \geq 0} b_{k,k'} X_0^{2k} X_1^{2k'+1}, \quad (48)$$

where $\alpha^2 = \lambda_0$, $s^2 \alpha^2 = \lambda_1$, and $a_{0,0} = b_{0,0} = 1$. As shown in Appendix D, the coefficients $a_{k,k'}$ and $b_{k,k'}$ are functions of s only and can be determined by recurrence relations. Imposing the boundary conditions at $u=0$: $\psi_0'(0)=0$ and $\psi_1(0)=0$ provide two equations independent of c and α

$$0 = \sum_{k,k' \geq 0} a_{k,k'} (2k+1+2k's) f_0^k f_1^{k'}, \quad (49)$$

$$0 = \sum_{k,k' \geq 0} b_{k,k'} f_0^k f_1^{k'}. \quad (50)$$

In practice the series are restricted to $k+k' \leq n$. At large enough n , for fixed s , this system of the variables $\{f_0, f_1\}$ has only one converging solution for positive f_0 and f_1 . The convergence with n depends on s . Relative convergence of 1% is reached at order $n \approx 40$. This slow convergence is due to the

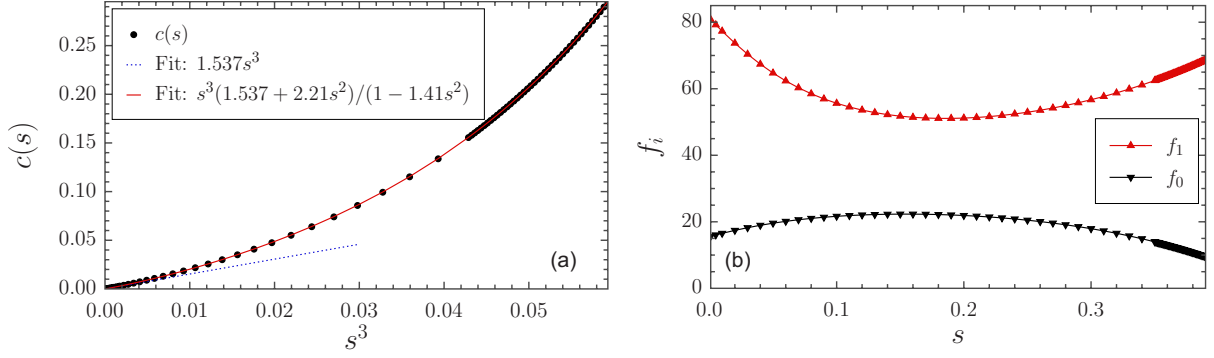


FIG. 3. (Color online) Graphical representation of the parameters for the two-mode model, see Eqs. (45) and (46), as functions of $s = \sqrt{\lambda_1/\lambda_0}$ with λ_i the eigenvalues of \mathcal{H}_0 , Eqs. (27). (a) Concentration $c \equiv c_1$ in the first-excited mode versus s^3 . (b) f_0 and f_1 versus s .

difficulty to fulfill the conditions at $u=0$ as we get close to the radius of convergence of these series. Machine precision is obtained using $n \approx 120$.

Then the normalizations of ψ_0 and ψ_1 lead to two simple equations determining α and c

$$\frac{1}{2} = \frac{\alpha^3}{1-c} \sum_{k,k' \geq 0} \frac{\rho_{k,k'}^{(0)} J_0^{k+1} J_1^k}{2(k+1+k's)}, \quad (51)$$

$$\frac{1}{2} = \frac{s^4 \alpha^3}{c} \sum_{k,k' \geq 0} \frac{\rho_{k,k'}^{(1)} J_0^k J_1^{k'+1}}{2[k+(k'+1)s]}, \quad (52)$$

where $\rho_{k,k'}^{(a)}$ is defined in Eq. (D2).

The variations in α are essentially linear and given by $\alpha = 0.4608 + 0.44c$ excepted at small c , where we add the residual correction: $10^{-3}(4.26 - 9.32c)/(1 + 41.5c)$. The variations in the other parameters are given in Fig. 3: c is essentially proportional to s^3 , f_0 , and f_1 vary within a factor of 2.

Within the Hartree approximation, \mathcal{E}_2^0 in Eq. (29) is still independent of r_s and of the polarization, p but depends on the concentration c . [see Fig. 4 (left)].

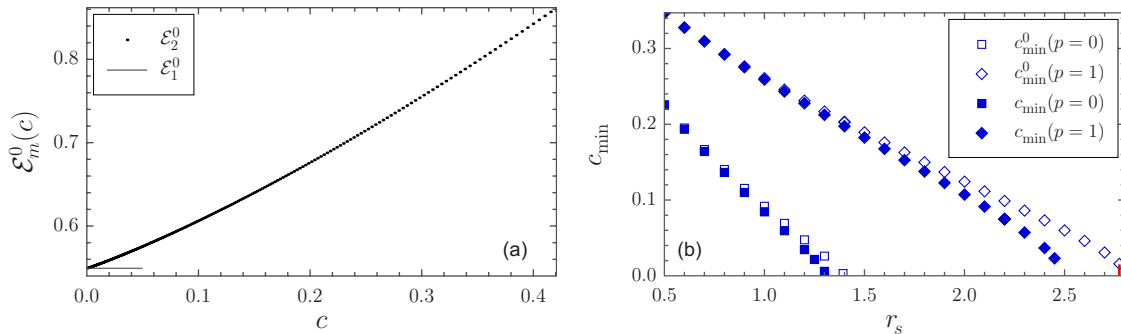


FIG. 4. (Color online) Two-mode model results. (a) Energy $\mathcal{E}_2^0(c)$ versus $c \equiv c_1$ the concentration in the first-excited state from Eq. (29) compared to the one-mode solution with $\mathcal{E}_1^0 \equiv \mathcal{E}_2^0(c=0)$. (b) Variations in the concentration c_{\min} , versus r_s that minimize E_2^0 of Eq. (54) (open symbols) or E_2 of Eq. (55) (full symbol). Squares (respectively, diamond) stand for the unpolarized (respectively, polarized) gas.

B. Two-mode exchange term with the Hartree approximation, \mathcal{X}_2^0

The two-mode exchange term for two modes reads

$$\mathcal{X}_2(c, r_s) = -\frac{r_s^{1/3}}{4\pi} \int_{\mathbb{R}} d\nu \left[\sum_{a=0}^1 |\tilde{\rho}_{aa}(\nu)|^2 c_a \tilde{Y}_1 \left(\frac{r_s^{1/3} G_p \nu}{\sqrt{c_a}} \right) + 2|\tilde{\rho}_{01}(\nu)|^2 \tilde{Y}_2(c, r_s^{1/3} G_p \nu) \right], \quad (53)$$

where $c_0 = 1 - c$ and $c_1 = c$. We refer to Appendix A for the definition and evaluation of the exchange integrals \tilde{Y}_1 and \tilde{Y}_2 , which have logarithmic singularities for small ν , and to Appendix B for the evaluation of the exchange term.

Using the Hartree approximation to determine the shape of the wave functions, the total two-mode energy is approximated by

$$E_2^0 = \frac{K_p[(1-c)^2 + c^2]}{r_s^2} + \frac{\mathcal{E}_2^0(c)}{r_s^{4/3}} + \frac{\mathcal{X}_2^0(c, r_s)}{r_s}. \quad (54)$$

At fixed r_s , a descent with respect to c allows us to determine the concentration c_{\min}^0 which minimizes $E_2^0(c)$. At small r_s , a minimum $c_{\min}^0 \neq 0$ is reached [see Fig. 4 (right)], and c_{\min}^0 decreases as r_s increases. The concentration in the excited mode vanishes at a critical value $r_{s,c} \approx 1.394(1)$ for the unpolarized gas. For the polarized gas, as r_s increases, $c=0$

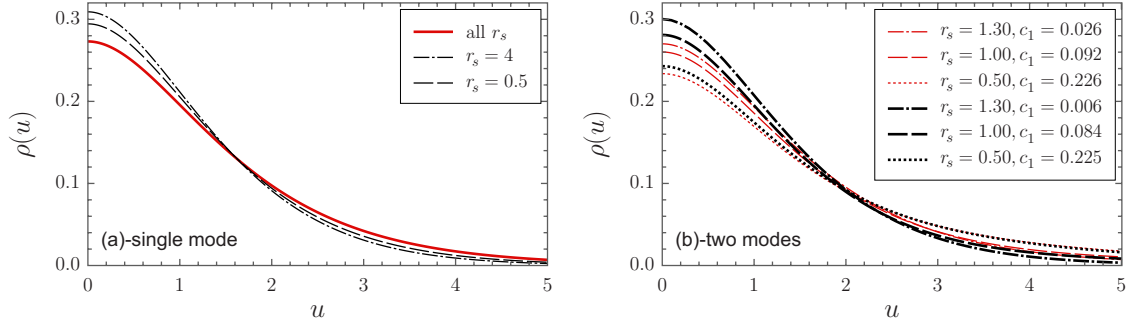


FIG. 5. (Color online) Comparison of the unpolarized charge-density profiles $\rho(u=r_s^{1/3}k_F z)$. Red lines stand for the analytical Hartree solutions, Eqs. (34) and (D1) while black lines stand for the optimized densities, as described in Secs. IV C and V C. In (b) c_1 is the first-excited-mode concentration minimizing the total energy; at this scale, the corrections coming from LDA-correlation energy are negligible (b). Notice that the red line at $r_s=1.3$ in (b), with a rather small value of c_1 is close to the red line in (a).

remains a local minimum. At $r_s=2.775$, the energy of the two-mode solution with $c_{\min}^0 \approx 0.015$ crosses the single-mode energy. Thus, within this approximation, we find a first-order transition for the polarized gas with a jump in the concentration [see Fig. 4 (right)].

C. Full minimization

The complete minimization of the total energy with two modes containing kinetic, Hartree, and exchange energy, is done by first finding the ground-state energy at fixed $\{r_s, c\}$ similar to the single-mode case

$$E_2 = \frac{K_p[(1-c)^2 + c^2]}{r_s^2} + \frac{\mathcal{E}_2(c, r_s)}{r_s^{4/3}} + \frac{\mathcal{X}_2(c, r_s)}{r_s}. \quad (55)$$

Then, at fixed r_s , the minimum, $c_{\min}(r_s)$, of the energy is found from a direct Newton descent on c . The variations in $c_{\min}(r_s)$ are close to $c_{\min}^0(r_s)$. They only differ significantly close to the transition. We find a transition at $r_{s,c}=1.30(1)$ for the unpolarized gas and $r_{s,c}=2.50(2)$ for the polarized gas. In particular, no first-order transition subsists for the polarized gas. The variations in the energy $E_2(c_{\min})$ versus r_s are close to $E_2^0(c_{\min}^0)$ (see Fig. 1).

D. Existence of three-mode solutions

We have further extended the method to study the occupation of three modes. Unfortunately, the series used for the Hartree approximation do not converge down to $u=0$. Nevertheless, the solution can be found numerically, and we find the three-mode solution more stable for $r_s < 0.75$ (respectively, $r_s < 1.6$) for the unpolarized (respectively, polarized) gas. Since the exchange contribution becomes less important for smaller r_s , we do not expect significant modifications from the full HF minimization.

Approaching the high-density limit, $r_s \rightarrow 0$, we expect an increasing number of occupied modes. For m modes, assuming $c_i=1/m$, the kinetic energy is $K_p/(mr_s^2)$, and the dimensionless Hartree energy is a function of m only, $\mathcal{E}_m^0(\{c_i=1/m\}) \equiv F(m)$, as can be seen from Eqs. (28) and (29). Minimizing the total energy, $E_m \approx K_p/(mr_s^2) + F(m)/r_s^{4/3}$, we can estimate the number of occupied modes in the high-density limit

$$m^2 F'(m) = K_p r_s^{-2/3}. \quad (56)$$

Assuming a linear behavior of F for large m , the number of occupied modes diverges as $r_s^{-1/3}$ as r_s approaches zero.

VI. CORRELATION ENERGY WITHIN THE LOCAL-DENSITY APPROXIMATION

Up to now, we have considered the total energy of the system within the Hartree-Fock approximation which neglects many-body correlation effects. Within density-functional theory (DFT), the correlation energy per particle for m modes, \mathcal{C}_m , defined as the difference between the true total energy and the best Hartree-Fock solution must be a functional of the electronic density only.⁶ Using the LDA,⁷ we can write

$$\mathcal{C}_m = \int_{\mathbb{R}} du \rho(u) \epsilon_c^{3D}[r_s^{3D}(u)], \quad (57)$$

where $\epsilon_c^{3D}[r_s^{3D}]$ is the correlation energy of the homogenous, three-dimensional electron gas at the (three-dimensional) density $n^{3D} a_B^3 = 3/(4\pi[r_s^{3D}]^3)$ expressed in terms of the three-dimensional electron-gas parameter r_s^{3D} . Using $n^{3D} = \sigma_0 \rho(u) du/dz$ we get $r_s^{3D}(u) = [3/8\rho(u)]^{1/3} r_s^{8/9}$. An estimation of the correlation effects is obtained by using the HF density, $\rho(u)$, of the one- and two-mode density distribution, together with the Perdew-Zunger⁸ parametrization of $\epsilon_c^{3D}[r_s^{3D}]$.

Around the transition between one and two excited modes of the unpolarized gas, $r_s \lesssim 1.3$, correlations, Eq. (57), lower the energy by typically less than 1%. Since the corresponding total density profiles (see Fig. 5) are smoothly varying with r_s and with the concentration in the first-excited state, c_1 , we do not expect important qualitative and quantitative modifications due to correlations in this density region. Energy minimizations including the LDA-correlation potential, $V_c[\rho(u)] = \delta \mathcal{C}_m / \delta \rho(u)$, in the effective Schrödinger equation, confirm that Hartree-Fock accurately describes the high-density region where the transition from single- to two-mode occupation of excited modes occurs.

VII. CONCLUSIONS

We have studied the model of a quasi-two-dimensional electron gas where electrons are confined by a positive charged background localized in the plane $z=0$. Similar to the 2DEG, the electronic density (r_s) is the only parameter of the system, however, the phase diagram is different due to possible transition from single- to multimode occupation in z . Here, we have restricted the discussion to the most simple phases in the metallic regime neglecting the possibility of charge ordering and Wigner crystallization.^{9,10} Already assuming a simple Fermi-liquid wave function in the high-density region, $r_s \rightarrow 0$, we have shown that a transition from a single to two or more occupied modes in the confined direction takes place. Indeed, we expect that close to $r_s=0$ three-dimensional features to be much more pronounced, as the dominant kinetic energy favors multimode occupations. Further, within HF, the transition between the polarized and unpolarized gas at $r_s \sim 4$ occurs in between the corresponding transitions of the 2DEG ($r_s \sim 2$) and the 3DEG ($r_s \sim 5$).¹¹ Similar to 2DEG and 3DEG, it is likely that the ferromagnetic phase of the Q2DEG is unstable against Wigner crystallization within HF, however correlations are expected to stabilize the ferromagnetic fluid phase in higher dimensions,^{3,12} so that the spin ordering of the Q2DEG may essentially differ from that of the 2DEG in the low-density region.

Within the Q2DEG, we expect that general aspects of the interplay between correlations and dimensionality can be studied without the need of a detailed microscopic modeling

of a particular experimental device. This is of particular importance since many experimental observations in quasi-two-dimensional electronic systems reflect strong correlation effects.¹³ Up to now, precise calculations of correlation effects using quantum Monte Carlo methods have mostly been done for the 2DEG (Refs. 2, 3, 5, and 14) but perturbative inclusion of the underlying third dimension have shown to introduce important quantitative changes, e.g., concerning the spin susceptibility.⁵ Within the Q2DEG model nonperturbative calculations are possible and phases not contained in the 2DEG can be observed. As a side effect, a quantitative study of the Q2DEG using quantum Monte Carlo methods, may also provide a reference system, which is strongly inhomogeneous in one direction, so that, within DFT, corrections to the local-density and generalized gradient approximations (GGAs) should be more pronounced, and functionals beyond LDA/GGA can be tested (see Ref. 15).

APPENDIX A: PROPERTIES OF THE EXCHANGE FUNCTION \tilde{Y}

The exchange function is given by the following integral:

$$\tilde{Y}(c_a, c_b, \nu) = \frac{2}{\pi^2} \int_{|k|^2 < c_a} d^2k \int_{|k'|^2 < c_b} d^2k' \frac{1}{(k-k')^2 + \nu^2}. \quad (\text{A1})$$

This function is positive for all ν , even in ν , and satisfies $\tilde{Y}(c_a, c_b, \nu) = \tilde{Y}(c_b, c_a, \nu)$ as well as $\alpha \tilde{Y}(\frac{c_a}{\alpha}, \frac{c_b}{\alpha}, \frac{\nu}{\alpha}) = \tilde{Y}(c_a, c_b, \nu)$. We find

$$\begin{aligned} \tilde{Y}(c_a, c_b, \nu) &= \frac{4}{\pi} \int_0^{\sqrt{c_a}} dk k \int_0^{\sqrt{c_b}} dk' k' \int_0^{2\pi} d\theta \frac{1}{k^2 + \nu^2 + k'^2 - 2kk' \cos(\theta)} \\ &= 8 \int_0^{\sqrt{c_a}} dk k \int_0^{\sqrt{c_b}} dk' k' \frac{1}{\sqrt{(k'^2 - k^2 + \nu^2)^2 + 4k^2\nu^2}} \\ &= 4 \int_0^{\sqrt{c_a}} dk k \left[\tanh^{-1} \frac{c_b + \nu^2 - k^2}{\sqrt{(k^2 - c_b + \nu^2)^2 + 4c_b\nu^2}} - \tanh^{-1} \frac{\nu^2 - k^2}{k^2 + \nu^2} \right] \\ &= 2 \int_0^{c_a} dk \left[\tanh^{-1} \frac{c_b + \nu^2 - k}{\sqrt{(k - c_b + \nu^2)^2 + 4c_b\nu^2}} - \frac{1}{2} \ln \frac{\nu^2}{k} \right] \\ &= X - c_a - c_b - \nu^2 + 2c_a \ln \frac{X - c_a + c_b + \nu^2}{2\nu^2} + 2c_b \ln \frac{X + c_a - c_b + \nu^2}{2\nu^2}, \end{aligned} \quad (\text{A2})$$

where

$$X = \sqrt{(\nu^2 + c_a + c_b)^2 - 4c_a c_b}. \quad (\text{A3})$$

In particular, within the context of the single-mode solution it is convenient to introduce the function $\tilde{Y}_1(\nu)$ given by

$$\tilde{Y}_1(\nu/\sqrt{c}) = \tilde{Y}(c, c, \nu)/c = \tilde{Y}(1, 1, \nu/\sqrt{c}),$$

$$\tilde{Y}_1(\nu) = 2t - 2 - 4 \ln t \quad \text{with} \quad t^{-1} = \frac{1}{2} + \frac{1}{2} \sqrt{1 + \frac{4}{\nu^2}},$$

(A4)

whereas for the two-mode model, we define $\tilde{Y}_2(\nu)$

$$\tilde{Y}_2(c, \nu) = \tilde{Y}(1 - c, c, \nu),$$

$$\begin{aligned} \tilde{Y}_2(c, \nu) = & X - 1 - \nu^2 + 2(1-c) \ln \frac{X + \nu^2 - 1 + 2c}{2\nu^2} \\ & + 2c \ln \frac{X + \nu^2 + 1 - 2c}{2\nu^2}. \end{aligned} \quad (\text{A5})$$

Both, \tilde{Y}_1 and \tilde{Y}_2 , have a logarithmic singularity at $\nu=0$ and behave as ν^{-2} at large ν ,

$$\tilde{Y}_1(\nu) = -2 - 4 \ln|\nu| + 4|\nu| + \mathcal{O}(\nu^2), \quad (\text{A6})$$

$$\begin{aligned} \tilde{Y}_2(c, \nu) = & -4c \ln|\nu| + 2[(1-c) \ln(1-c) - (1-2c) \\ & \times \ln(1-2c) - c] + \mathcal{O}(\nu^2), \end{aligned} \quad (\text{A7})$$

$$\tilde{Y}_1(\nu) = \frac{2}{\nu^2} - \frac{2}{\nu^4} + \mathcal{O}(\nu^{-6}), \quad (\text{A8})$$

$$\tilde{Y}_2(c, \nu) = \frac{2c(1-c)}{\nu^2} - \frac{c(1-c)}{\nu^4} + \mathcal{O}(\nu^{-6}). \quad (\text{A9})$$

APPENDIX B: EVALUATION OF THE EXCHANGE TERM

For the one-mode exchange term of the energy, \mathcal{X}_1 , we need to evaluate the following integral:

$$\mathcal{X}_1 = -\frac{\beta}{2\pi} \int_0^\infty d\nu \tilde{\rho}(\nu)^2 \tilde{Y}_1(G_p \beta \nu), \quad (\text{B1})$$

where $\beta = r_s^{1/3}$ and $\tilde{\rho}(\nu)$ is the Fourier transform of $\rho(u)$. For \mathcal{X}_1^0 , the density is defined in Eq. (34) and $\tilde{\rho}(\nu)$ can be computed from

$$\begin{aligned} \tilde{\rho}(\nu) = & 2 \int_0^\infty du \rho(u) \cos(\nu u) \\ = & 2\alpha^4 \sum_{k \geq 0} (-1)^k j_0^{k+1} \rho_k \frac{2(k+1)\alpha}{4(k+1)^2 \alpha^2 + \nu^2}. \end{aligned} \quad (\text{B2})$$

To remove the logarithmic singularity of the integrand at $\nu=0$, we introduce an auxiliary function e_1 ,

$$\begin{aligned} \mathcal{X}_1 = & -\frac{1}{2\pi} \left\{ e_1(\beta, \tau) + \int_0^\infty d\nu [\tilde{\rho}(\nu)^2 \beta \tilde{Y}_1(G_p \beta \nu) \right. \\ & \left. - \tilde{e}_1(\nu, \beta, \tau) \right\}, \end{aligned} \quad (\text{B3})$$

with

$$\tilde{e}_1(\nu, \beta, \tau) = [e^{-\tau\nu}(1 + \tau\nu)]^2 \beta [-4 \ln(G_p \beta \nu) - 2 + 4G_p \beta \nu], \quad (\text{B4})$$

$$\begin{aligned} e_1(\beta, \tau) = & \int_0^\infty d\nu \tilde{e}_1(\nu, \beta, \tau) = \frac{9G_p \beta^2}{2\tau^2} \\ & + \frac{\beta}{\tau} \left(-6 + 5 \ln \frac{2\tau}{G_p \beta} + 5\gamma \right), \end{aligned} \quad (\text{B5})$$

where γ is the Euler constant and $\tau = \sqrt{2\tilde{\rho}^{(2)}}$ is determined

from $\tilde{\rho}(\nu) = 1 - \rho^{(2)} \nu^2 + \mathcal{O}(\nu^4)$ [$\rho^{(2)} = 1.617362956587058$ using the solution of Eq. (34)]. The integral in Eq. (B3) is then free of singularities and can be evaluated without major difficulties.

Calculating the first integral in Eq. (53) contributing to the exchange term of two modes, \mathcal{X}_2 , we adapt the above procedure for the integrals involving $\tilde{\rho}_{aa}$ using $\tilde{e}_2(\nu, \tau)$,

$$\begin{aligned} \tilde{e}_2(\nu, \beta, \tau, c) = & [e^{-\tau\nu}(1 + \tau\nu)]^2 c \beta [-4 \ln(G_p \beta \nu / \sqrt{c}) - 2 \\ & + 4G_p \beta \nu / \sqrt{c}], \end{aligned} \quad (\text{B6})$$

$$e_2(\beta, \tau, c) = c^{3/2} e_1(\beta, \tau \sqrt{c}). \quad (\text{B7})$$

The logarithmic singularity in the second contribution containing \tilde{Y}_2 in Eq. (53) is cancelled by $\tilde{\rho}_{ab}(\nu)$ which is proportional to ν at small ν .

Similar auxiliary functions are used to evaluate $V_{aa}^{\text{exc}}(u)$ whereas the logarithm singularity of $\tilde{Y}_2(\nu, c)$ in $V_{ab}^{\text{exc}}(u)$ is again cancelled by $\tilde{\rho}_{ab}(\nu) \propto \nu$.

APPENDIX C: DETAILS ON THE NUMERICAL MINIMIZATION SCHEME

Here, we describe some details on the numerical minimization of the total Hartree-Fock energy, Eq. (19). For simplicity, we restrict the discussion to the single-mode solution where the formal derivative is given by $d\psi = \mathcal{H}_d \psi$ ($\mathcal{H}_d = 4\mathcal{H}_0/r_s^{4/3} + 4V_{00}/r_s$). We proceed using a quadratic minimization scheme. Let $\psi^{(n)}$ be the solution at step n and $\{d\psi^{(n-1)}, d\psi^{(n)}\}$ the derivatives at step $n-1$ and n . Energies $E(\varepsilon_1, \varepsilon_2)$ are computed at $\psi^{(n)} + \varepsilon_1 d\psi^{(n-1)} + \varepsilon_2 d\psi^{(n)}$ for the six points $(\varepsilon_1, \varepsilon_2) = (0, 0), (\pm \epsilon, 0), (0, \pm \epsilon)$, and $(\epsilon, -\epsilon)$. By assuming a second-order polynomial in ε_1 and ε_2 , the minimum of $E(\varepsilon_1, \varepsilon_2)$ is determined analytically and defines the solution at step $n+1$.

All functions of u , e.g., $\psi(u)$, are computed on a grid of 2^p points $(i - i_0 + 1)\delta$ with i from 0 to $2^p - 1$, $i_0 = 2^{p-1}$ and $\delta = u_{\text{max}}/i_0$. Fast Fourier transform are used to compute $\tilde{\rho}(\nu)$. In order to achieve good convergence small values of δ are needed to accurately calculate the kinetic energy of the direct (Hartree) potential whereas a small step in ν is needed for the exchange energy which implies large values of u_{max} . We found that $u_{\text{max}} = 150$ and $p = 10$ are good starting values at sufficiently large value of c . At small c , the spatial extension of the excited mode increases significantly which prevents accurate solutions for $c \lesssim 10^{-3}$. Interpolating $\psi(u)$ allows us to increase p at fixed u_{max} .

APPENDIX D: RECURRENCE RELATION FOR THE TWO-MODE HARTREE SOLUTION

We determine the recurrence relation of the series coefficients in the two-mode case. The densities are given by

$$\rho = \alpha^4 \sum_{k, k' \geq 0} \rho_{k, k'} X_0^{2k} X_1^{2k'} \quad \rho_{k, k'} = \rho_{k-1, k'}^{(0)} + s^4 \rho_{k, k'-1}^{(1)}, \quad (\text{D1})$$

$$\rho_{k,k'}^{(0)} = \sum_{j=0}^k \sum_{j'=0}^{k'} a_{j,j'} a_{k-j,k'-j'}, \quad \rho_{k,k'}^{(1)} = \sum_{j=0}^k \sum_{j'=0}^{k'} b_{j,j'} b_{k-j,k'-j'}, \quad (\text{D2})$$

with the convention that $a_{-1,k'} = b_{k,-1} = 0$, and the potential is defined as

$$v_\rho(u) = -\alpha^2 \sum_{k,k' \geq 0} v_{k,k'} X_0^{2k} X_1^{2k'} \quad \text{with} \quad v_{k,k'} = \frac{\rho_{k,k'}}{4(k+k's)^2}. \quad (\text{D3})$$

We have

$$v_\rho \psi_0 = -\frac{\alpha^4}{\sqrt{1-c}} \sum_{k,k' \geq 0} w_{k,k'} X_0^{2k+1} X_1^{2k'}$$

with

$$w_{k,k'} = \sum_{j=0}^k \sum_{j'=0}^{k'} v_{j,j'} a_{k-j,k'-j'}, \quad (\text{D4})$$

$$v_\rho \psi_1 = -\frac{s^2 \alpha^4}{\sqrt{c}} \sum_{k,k' \geq 0} w'_{k,k'} X_0^{2k} X_1^{2k'+1}$$

with

$$w'_{k,k'} = \sum_{j=0}^k \sum_{j'=0}^{k'} v_{j,j'} b_{k-j,k'-j'}. \quad (\text{D5})$$

Imposing $\psi_0'' - (v_\rho + \alpha^2)\psi_0 = 0$ and $\psi_1'' - (v_\rho + s\alpha^2)\psi_1 = 0$ gives

$$\sum_{k,k' \geq 0} a_{k,k'} [(2k+1+2k's)^2 - 1] X_0^{2k+1} X_1^{2k'} + \sum_{k,k' \geq 0} w_{k,k'} X_0^{2k+1} X_1^{2k'} = 0, \quad (\text{D6})$$

$$\sum_{k,k' \geq 0} b_{k,k'} \{[2k + (2k'+1)s]^2 - s^2\} X_0^{2k} X_1^{2k'+1} + \sum_{k,k' \geq 0} w_{k,k'} X_0^{2k} X_1^{2k'+1} = 0, \quad (\text{D7})$$

with the following solution for $(k,k') \neq (0,0)$:

$$a_{k,k'} = -\frac{w_{k,k'}}{4(k+k's)(k+1+k's)}, \quad (\text{D8})$$

$$b_{k,k'} = -\frac{w'_{k,k'}}{4(k+k's)[k+(k'+1)s]}. \quad (\text{D9})$$

Thus, the coefficients $a_{k,k'}$ and $b_{k,k'}$, as well as $\rho_{k,k'}$ and $v_{k,k'}$, are rational functions of s only.

¹A. K. Rajagopal and J. C. Kimball, *Phys. Rev. B* **15**, 2819 (1977).

²B. Tanatar and D. M. Ceperley, *Phys. Rev. B* **39**, 5005 (1989).

³N. D. Drummond and R. J. Needs, *Phys. Rev. Lett.* **102**, 126402 (2009).

⁴T. Ando, A. B. Fowler, and F. Stern, *Rev. Mod. Phys.* **54**, 437 (1982).

⁵S. De Palo, M. Botti, S. Moroni, and G. Senatore, *Phys. Rev. Lett.* **94**, 226405 (2005).

⁶P. Hohenberg and W. Kohn, *Phys. Rev.* **136**, B864 (1964).

⁷W. Kohn and L. J. Sham, *Phys. Rev.* **140**, A1133 (1965).

⁸J. P. Perdew and A. Zunger, *Phys. Rev. B* **23**, 5048 (1981).

⁹E. P. Wigner, *Trans. Faraday Soc.* **34**, 678 (1938); *Phys. Rev.*

46, 1002 (1934).

¹⁰B. Bernu, F. Delyon, M. Duneau, and M. Holzmann, *Phys. Rev. B* **78**, 245110 (2008).

¹¹J. R. Trail, M. D. Towler, and R. J. Needs, *Phys. Rev. B* **68**, 045107 (2003).

¹²L. Cândido, B. Bernu, and D. M. Ceperley, *Phys. Rev. B* **70**, 094413 (2004).

¹³B. Spivak, S. V. Kravchenko, S. A. Kivelson, and X. P. A. Gao, *Rev. Mod. Phys.* **82**, 1743 (2010).

¹⁴M. Holzmann, B. Bernu, V. Olevano, R. M. Martin, and D. M. Ceperley, *Phys. Rev. B* **79**, 041308(R) (2009).

¹⁵Y. H. Kim, I. H. Lee, S. Nagaraja, J. P. Leburton, R. Q. Hood, and R. M. Martin, *Phys. Rev. B* **61**, 5202 (2000).